Internal Gravity Waves

Bruce R. Sutherland
4-183 CCIS, Dept. Physics
University of Alberta
Edmonton, AB   T6G 2E1
Canada
Email: bruce.sutherland@ualberta.ca
Tel: +1 (780) 492-0573

1   INTRODUCTION

Ocean waves move due to gravity: the water at crests is heavier than the air surrounding it and so it falls, overshoots its equilibrium position and then at a trough feels an upward restoring force. The same phenomena occurs below the ocean surface. Cold water lifted upward into warmer surroundings will feel a downward buoyancy force and downward-displaced warm water will feel an upward buoyancy force. If this motion is periodic in both space and time, it is referred to as an internal gravity wave. Internal gravity waves are manifest in two qualitatively different forms, which we will refer to here as "interfacial waves" and "internal waves". (The dynamics of internal waves are broadly discussed in the textbook "Internal Gravity Waves" (Sutherland 2010)).

Interfacial waves exist at the interface between dense and less dense fluid such as the thermocline, which refers to the interface between warm and cold water, or an atmospheric inversion, which refers to the interface between warm and cold air. In the ocean and in laboratory experiments, they can also exist at a halocline, which is the interface between fresh and salty water. An example of such a wave is shown in Figure 1a, in which a subsurface disturbance has launched a wave beneath a nearly flat surface. Looking down on the surface, the presence of these waves is evident from fluctuating horizontal flows and, on large scales, changing surface roughness.

Large-amplitude interfacial waves at the thermocline in the ocean and launched onto the continental shelf by tides provide enhanced transport of fluid and biology. For this reason, they are of interest to marine biologists, sediment geologists as well as theoretical modellers.

The second form of internal gravity wave exists in continuously stratified fluid, which means that the effective density of the fluid gradually decreases with height. These waves again move up and down due to buoyancy, but they are not confined to an interface; they can move vertically as well as horizontally through the fluid. These are shown in Figure 1b in which model hills create a perturbation that launches waves moving upward through the fluid whose density decreases linearly with height as the salinity decreases.

Though not of primary importance, internal waves have a non-negligible influence upon weather and climate through the vertical transport of energy and momentum. In the atmosphere, for example, the waves launched by flow over mountains exert drag on the air far above where they break. In the ocean, wave breaking is a source of deep-ocean mixing, which is an important means of vertically redistributing heat. On the mesoscale, breaking
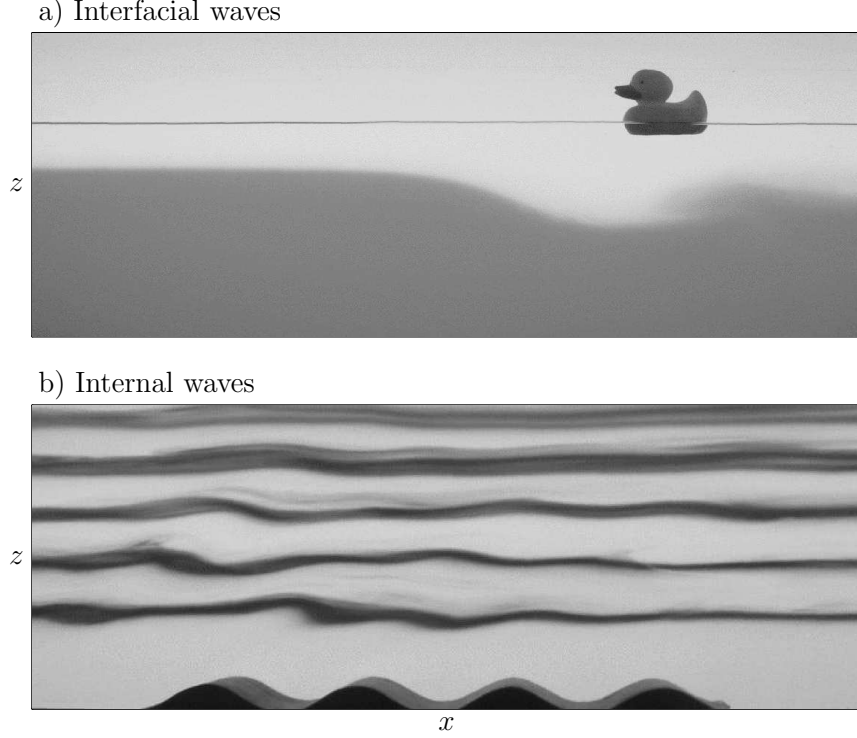
a) Interfacial waves

b) Internal waves

Figure 1: a) Laboratory experiment in which the interface between (dark-dyed) salty fluid and (clear) fresh water is displaced by an interfacial internal wave that passes beneath a nearly flat surface. b) Laboratory experiment in which towed model-hills launch vertically propagating internal waves in continuously stratified fluid. The waves are visualized by the displacement of dye-lines equally spaced by 5cm.

large-amplitude internal waves are a source of clear-air-turbulence, which is a threat to air traffic.

The properties of periodic small-amplitude interfacial and internal waves is well-established but less is known about the dynamics of large-amplitude waves. In this chapter, we will review the theory of these two types of waves having small and moderately large amplitude. The waves that influence the environment occur on small spatial and fast temporal scales, so that the effects of the Earth's rotation can be ignored.

2 EQUATIONS DESCRIBING INTERFACIAL WAVES

We will consider the propagation of interfacial waves in a two-layer fluid of upper depth H_1 and lower depth H_2, as shown in Figure 2. The density, ρ_1, of the upper layer is assumed to be moderately smaller than the lower-layer density, ρ_2. This allows us to make the Boussinesq approximation, in which the density affects buoyancy forces but not the momentum of the fluid.

An unsheared uniform density, Boussinesq fluid is irrotational and incompressible. This means that the velocity everywhere in the fluid can be prescribed in terms of gradients of
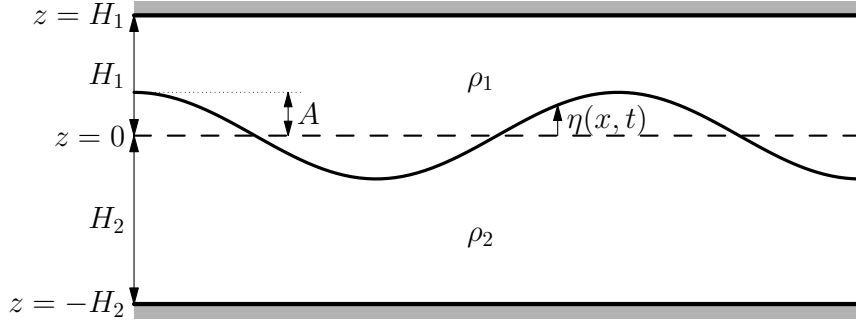
Figure 2: Schematic showing the definition of variables and scales used to model interfacial waves.

a velocity potential, $\phi(x, z, t)$, so that

$$(u, w) = \left(\frac{\partial \phi}{\partial x}, \frac{\partial \phi}{\partial x} \right). \tag{1}$$

and ϕ itself satisfies

$$\frac{\partial^2 \phi}{\partial x^2} + \frac{\partial^2 \phi}{\partial z^2} = 0. \tag{2}$$

Insisting that the vertical velocity field is zero at the upper and lower boundaries, we also have the conditions

$$\left. \frac{\partial \phi}{\partial z} \right|_{z=-H_2} = \left. \frac{\partial \phi}{\partial z} \right|_{z=H_1} = 0. \tag{3}$$

The physics of buoyancy forces that drives the waves are included in interface conditions. Before invoking these, we can make some progress in solving the boundary value problem (2) with (3). Seeking solutions that are periodic in horizontal space and in time, we assume $\phi(x, z, t) = \hat{\phi}(z) \sin(kx - \omega t)$, in which $k = 2\pi/\lambda$ is the horizontal wavenumber for waves with wavelength λ and $\omega = 2\pi/T$ is the frequency for waves with period T. Substituting this expression into (2) is equivalent to a Fourier Sine transform. Thus we get an ordinary differential equation for $\hat{\phi}$:

$$-k^2 \hat{\phi} + \frac{d^2 \hat{\phi}}{dz^2} = 0. \tag{4}$$

General solutions are a superposition of the exponential functions e^{kz} and e^{-kz}. The particular combination of these functions that satisfies the boundary conditions (3) is written succinctly in terms of the hyperbolic cosine ($\cosh(\theta) = (e^\theta + e^{-\theta})/2$):

$$\phi = \begin{cases} A_1 \cosh[k(z - H_1)] \sin(kx - \omega t) & z > 0 \\ A_2 \cosh[k(z + H_2)] \sin(kx - \omega t) & z < 0 \end{cases}. \tag{5}$$

Here we have assumed the amplitude of the waves is so small that it is sufficient to define ϕ above and below $z = 0$ rather than above and below the displaced interface at $z = \eta$. There is virtually no difference between $\phi(x, \eta, t)$ and $\phi(x, 0, t)$ as η goes to zero.
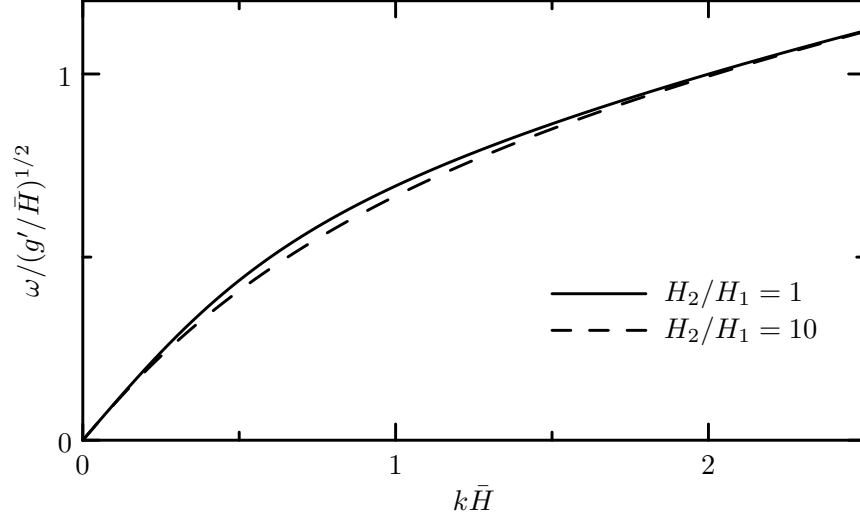
3

Figure 3: Plot of dispersion relation (9) for small-amplitude interfacial waves with $H_2/H_1 = 1$ and $H_2/H_1 = 10$ (or, equivalently $H_1/H_2 = 10$). Frequency is normalized by its characteristic value $\sqrt{g'/\bar{H}}$ and wavenumber by its characteristic value $1/\bar{H}$ in which $\bar{H} = H_1 H_2/(H_1 + H_2)$ is the harmonic mean of the depths of the upper and lower layer fluids.

Our problem reduces to finding the connection between the amplitudes A_1 and A_2 of the velocity potential in the upper and lower fluids as well as connecting these to the amplitude (and structure) of the interfacial displacement η.

The effects of buoyancy forces driving the wave motion are accounted for by Bernouilli's condition that $\rho(\partial_t \phi + \frac{1}{2}|\vec{u}|^2 + g\eta)$ should not change across the interface. That is, there is no pressure jump across the interface. For small-amplitude waves, we can neglect the small kinetic energy term. Therefore, using (5) and evaluating ϕ at the height of the interface where $z \simeq 0$, we have

$$\eta(x,t) = -\frac{\omega}{g'}\left(A_1 \cosh(kH_1) - A_2 \cosh(kH_2)\right)\cos(kx - \omega t), \tag{6}$$

in which we have defined the reduced gravity to be $g' \equiv g(\rho_2 - \rho_1)/\rho_2$.

Another condition at the interface requires that their should be no jump in the vertical velocity, $w = \partial_z \phi$, across it. From (5), this relates the values A_1 and A_2 for small amplitude waves by the condition

$$-A_1 \sinh(kH_1) = A_2 \sinh(kH_2), \tag{7}$$

in which $\sinh\theta = (e^\theta - e^{-\theta})/2$ is the hyperbolic sine function. The vertical velocity field is also given in terms of the interface displacement for small-amplitude waves by $\partial_t \eta$. And so we have a second equation relating A_1 and A_2. Using (6) to equate $\partial_t \eta$ to $\partial_z \phi$ just above the interface gives

$$\frac{\omega^2}{g'}\left(A_1 \cosh(kH_1) - A_2 \cosh(kH_2)\right) = kA_1 \sinh(kH_1). \tag{8}$$

4

	General formula	Long wave limit $(k\bar{H} \ll 1)$
$\eta =$	$A\cos(kx - \omega t)$	$\to A\cos(kx - \omega t)$
$\phi =$	$\begin{cases} -A\,\frac{\omega}{k}\frac{\cosh[k(z-H_1)]}{\sinh(kH_1)}\sin(kx-\omega t) \\ A\,\frac{\omega}{k}\frac{\cosh[k(z+H_2)]}{\sinh(kH_2)}\sin(kx-\omega t) \end{cases}$	$\to \begin{cases} -A\,\frac{\omega}{k^2 H_1}\sin(kx-\omega t) & z>0 \\ A\,\frac{\omega}{k^2 H_2}\sin(kx-\omega t) & z<0 \end{cases}$
$u =$	$\begin{cases} -A\,\omega\frac{\cosh[k(z-H_1)]}{\sinh(kH_1)}\cos(kx-\omega t) \\ A\,\omega\frac{\cosh[k(z+H_2)]}{\sinh(kH_2)}\cos(kx-\omega t) \end{cases}$	$\to \begin{cases} -A\,\frac{\omega}{kH_1}\cos(kx-\omega t) & z>0 \\ A\,\frac{\omega}{kH_2}\cos(kx-\omega t) & z<0 \end{cases}$
$w =$	$\begin{cases} -A\,\omega\frac{\sinh[k(z-H_1)]}{\sinh(kH_1)}\sin(kx-\omega t) \\ A\,\omega\frac{\sinh[k(z+H_2)]}{\sinh(kH_2)}\sin(kx-\omega t) \end{cases}$	$\to \begin{cases} -A\,\omega\left(\frac{z}{H_1}-1\right)\sin(kx-\omega t) & z>0 \\ A\,\omega\left(\frac{z}{H_2}+1\right)\sin(kx-\omega t) & z<0 \end{cases}$
$\xi =$	$\begin{cases} -A\,\frac{\sinh[k(z-H_1)]}{\sinh(kH_1)}\cos(kx-\omega t) \\ A\,\frac{\sinh[k(z+H_2)]}{\sinh(kH_2)}\cos(kx-\omega t) \end{cases}$	$\to \begin{cases} -A\,\left(\frac{z}{H_1}-1\right)\cos(kx-\omega t) & z>0 \\ A\,\left(\frac{z}{H_2}+1\right)\cos(kx-\omega t) & z<0 \end{cases}$

Table 1: Relationships between the interface displacement (η), velocity potential (ϕ), the horizontal (u) and vertical (w) components of velocity, and the vertical displacement field for interfacial waves in general and in the long wave limit.

Eliminating A_2 from (7) and (8) gives a single equation for A_1:

$$A_1 \sinh(kH_1)\left[\frac{\omega^2}{g'}\left(\frac{\cosh(kH_1)}{\sinh(kH_1)} + \frac{\cosh(kH_2)}{\sinh(kH_2)}\right) - k\right] = 0.$$

Because we are assuming A_1, k and H_1 are non-zero, we must have that the expression in square brackets is zero.

Thus we have determined the dispersion relation for an interfacial waves:

$$\omega^2 = g'k[\coth(kH_1) + \coth(kH_2)]^{-1}, \tag{9}$$

in which we have introduced the hyperbolic cotangent. This is plotted in Figure 3. Effectively we have just solved an eigenvalue problem. In its solution we have found that the frequency of the wave depends upon the wavenumber k. For a given value of the amplitude A_1, we can then find the value of A_2 through (7) and so find interfacial displacement (6). These and other polarization relations are listed in Table 1 in which the results have been recast to represent the relationship between fields in terms of the interfacial displacement amplitude A such that $\eta = A\cos(kx - \omega t)$.

Of particular interest is the properties of waves that are long compared to the fluid depth, so that both kH_1 and kH_2 are small. These are called "shallow water waves". For small θ, $\coth\theta \simeq 1/\theta$. So the general dispersion relation (9) becomes In the limit of small kH_1 and kH_2 are small

$$\omega^2 = c^2 k^2 \tag{10}$$

in which $c = \sqrt{g'\bar{H}}$ and $\bar{H} = H_1 H_2/(H_1 + H_2)$ is the harmonic mean of the two depths. So long waves are non-dispersive: all wavelengths travel at the same phase and group speed, c.
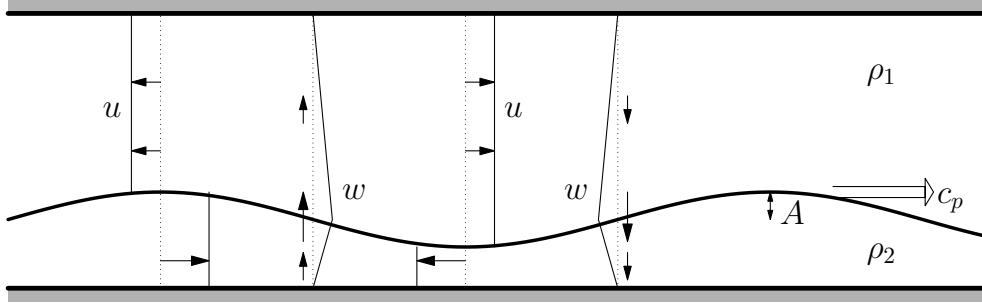
5

Figure 4: Schematic showing the velocity fields associated with a rightward-propagating shallow interfacial wave in a two-layer fluid. Here $H_1 = 0.75H$ and $H_2 = 0.25H$. For clarity of the illustration, the displacement amplitude has been exaggerated, though in reality such a value of A would constitute a large-amplitude interfacial wave.

In the shallow-water limit the horizontal velocity is uniform within each layer but moves in opposite directions above and below the interface, as shown in Figure 4. The presence of shear at the interface suggests the possibility of breakdown into turbulence for sufficiently large amplitude waves (Troy and Koseff 2005). The vertical velocity changes linearly within each layer having maximum upward velocity at the inflection point leading the crest.

3   EQUATIONS DESCRIBING INTERNAL WAVES

Although it is often mathematically convenient to represent the thermocline as a sharp interface, for many wave phenomena the details of the ambient vertical density profile non-negligibly affect the structure and evolution of internal waves. In the extreme case of a uniformly stratified fluid, in which the density decreases linearly with height, the ambient fluid is no longer irrotational because the density gradients introduce vorticity within the ambient through so-called baroclinic torques.

The evolution of Boussinesq internal waves in the x-z plane is governed by the conservation of momentum and internal energy for an incompressible fluid:

$$\rho_0 \frac{Du}{Dt} = -\frac{\partial p}{\partial x} \tag{11}$$

$$\rho_0 \frac{Dw}{Dt} = -\frac{\partial p}{\partial z} - g\rho \tag{12}$$

$$\frac{D\rho}{Dt} = -w\frac{d\bar{\rho}}{dz} \tag{13}$$

$$\frac{\partial u}{\partial x} + \frac{\partial w}{\partial z} = 0, \tag{14}$$

in which ρ_0 is the characteristic density, $\bar{\rho}(z)$ is the ambient density and ρ is the fluctuation density resulting from the passage of waves. We have assumed there is no background flow so that the horizontal motion u is entirely due to waves.

If the waves are small amplitude, we may neglect the advective terms in the material derivative and so replace D/Dt with $\partial/\partial t$. The equations can then be combined into a

	Modes	Vertically Propagating Waves
$\xi =$	$A \sin(m_i z) \cos(kx - \omega t)$	$A \cos(kx + mz - \omega t)$
$\psi =$	$-A \frac{\omega}{k} \sin(m_i z) \cos(kx - \omega t)$	$-A \frac{\omega}{k} \cos(kx + mz - \omega t)$
$u =$	$-A \frac{\omega m_i}{k} \cos(m_i z) \sin(kx - \omega t)$	$-A \frac{\omega m}{k} \sin(kx + mz - \omega t)$
$w =$	$A \omega \sin(m_i z) \cos(kx - \omega t)$	$A \omega \sin(kx + mz - \omega t)$

Table 2: Relationships between the isopycnal displacement (ξ), streamfunction (ψ) and the horizontal (u) and vertical (w) components of velocity for internal wave modes in a uniformly stratified fluid in a channel with $0 \leq z \leq H$ and for vertically propagating internal waves in an unbounded domain. The i-th vertical mode has vertical wavenumber $m_i = i\pi/H$ for positive integers i.

single equation in one variable. Because the fluid is incompressible, we may define the streamfunction ψ so that $u = -\partial_z \psi$ and $w = \partial_x \psi$. Putting this into the momentum equations, taking the curl to eliminate pressure and finally eliminating ρ, we have the following:

$$\frac{\partial^2}{\partial t^2} \left(\frac{\partial^2}{\partial x^2} + \frac{\partial^2}{\partial z^2} \right) \psi + N^2 \frac{\partial^2}{\partial x^2} \psi = 0, \tag{15}$$

in which $N^2(z) = -(g/\rho_0)d\bar{\rho}/dz$ is the squared buoyancy frequency.

We seek solutions that are periodic in horizontal space and time and so write $\psi(x, z, t) = \hat{\psi}(z) \cos(kx - \omega t)$. Substituting this into (15) gives the equation describing the vertical structure of the waves:

$$\frac{d^2\hat{\psi}}{dz^2} + k^2 \left(\frac{N^2}{\omega^2} - 1 \right) \hat{\psi} = 0. \tag{16}$$

The structure is oscillatory in z where $\omega < N$ and changes exponentially in z where $\omega > N$. For given ω and k the solution depends upon the upper and lower boundary conditions as well as the prescribed value of $N(z)$.

In a uniformly stratified fluid ($N = N_0$, constant) explicit analytic solutions can be found: $\hat{\psi}$ is the superposition of the functions $\sin(mz)$ and $\cos(mz)$ in which

$$m = k(N_0^2/\omega^2 - 1)^{1/2}. \tag{17}$$

In an unbounded fluid it is usual to form the superposition so that the streamfunction describes waves either with upward moving crests, $\psi(x, z, t) = A_{\psi+} \cos(kx + mz - \omega t)$, or with downward moving crests, $\psi(x, z, t) = A_{\psi-} \cos(kx - mz - \omega t)$. If the fluid is bounded above and below by horizontal boundaries, the superposition must be taken to ensure no vertical motion at top and bottom:

$$\psi(x, z, t) = A_{\psi i} sin(m_i z) \cos(kx - \omega t), \quad i = 1, 2, 3, \ldots \tag{18}$$

in which the domain is assumed to extend from 0 to H and $m_i = i\pi/H$ for positive integers i ensures that ψ, and hence, w is zero at $z = 0$ and H.
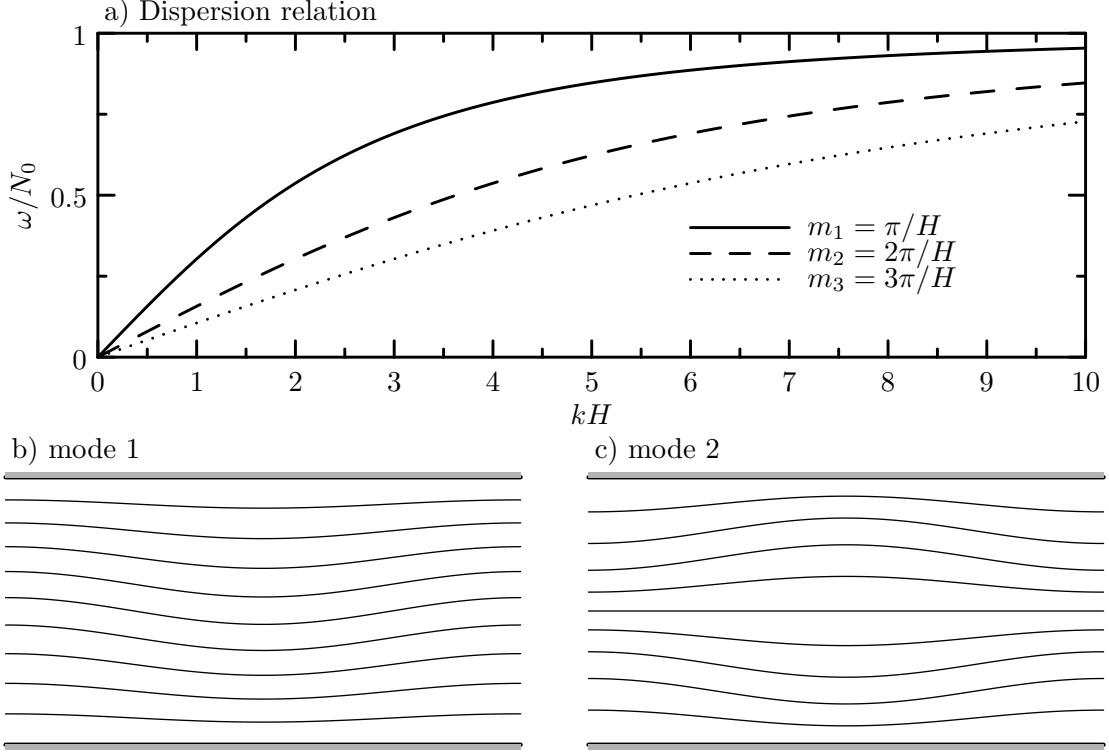
Figure 5: a) Dispersion relation of lowest three vertical modes of internal waves in uniformly stratified fluid with buoyancy frequency N_0 in a domain of depth H. Isopycnal displacements are shown for b) mode-1 and c) mode-2 waves.

In either case, the dispersion relation for internal waves in uniformly stratified fluid is given by rearranging (17) to isolate ω:

$$\omega^2 = N_0{}^2 \frac{k^2}{k^2 + m^2} \tag{19}$$

in which m varies continuously for waves in an unbounded domain but is discrete-valued in a vertically finite domain. Whereas there is a single dispersion relation for interfacial waves with given k, internal waves have an infinite set of dispersion relations depending upon the value of m.

For a given mode, we may go on to find the velocity fields and other fields of interest. In particular, the vertical ($\hat{w}$) and horizontal ($\hat{u}$) velocities are proportional to $\hat{\psi}$. These polarization relations are listed in Table 2. For comparison with the polarization for interfacial waves, listed in Table 1, these have been cast in terms of the amplitude, A, of the vertical displacement field. This is the maximum displacement of isopycnals in the domain.

The dispersion relation for internal waves in a fluid of finite depth is shown in Figure 5a. The corresponding structure of the lowest two vertical modes is illustrated in Figures 5b and c through lines indicating the isopycnal displacements at snapshot in time.

For all vertical modes, the waves become non-dispersive in the limit of long horizontal waves for which $k \ll m_i$. In this case the horizontal phase and group speed associated with

8

the waves is $c = N_0/m_i = N_0 H/(i\pi)$ for positive integers, i. The fastest speed is associated with the lowest $(i = 1)$ mode.

The velocity fields associated with the mode-1 internal wave is illustrated in Figure 6. Here the thick black lines represent four initially evenly spaced isopycnals (lines of constant density) which have been lifted upward and downward from their equilibrium positions due to the passage of the waves. In an unbounded stratified fluid, the vertical and horizontal velocity fields associated with a plane wave are in phase. However, as with interfacial waves, the velocity fields of bounded internal wave modes are 90° out of phase. Comparing this figure with Figure 4, we see that the most significant qualitative difference is that u varies continuously with z and w varies smoothly with z.

We can draw the connection between interfacial waves and vertically bounded internal waves by considering modes in a cavity with ambient density given by

$$\bar{\rho}(z) = \begin{cases} \rho_1 & \sigma H_1 < z \le H_1 \\ \frac{\rho_1 H_2 + \rho_2 H_1}{H} - \frac{\rho_2 - \rho_1}{\sigma H} z & -\sigma H_2 \le z \le \sigma H_1 \\ \rho_2 & -\sigma H_2 > z \ge -H_2 \end{cases} \qquad (20)$$

in which $H = H_1 + H_2$ is the total fluid depth and σ is a measure of the interface thickness. We recover the case of interfacial waves in the limit $\sigma \to 0$ and we recover the case of internal waves in uniformly stratified fluid as $\sigma \to 1$. The corresponding N^2 profile is zero in the upper and lower layers and holds the constant value

$$N_0 = \sqrt{\frac{g}{\rho_0} \frac{\rho_2 - \rho_1}{\sigma H}} = \sqrt{\frac{g'}{\sigma H}}, \qquad (21)$$

for $-\sigma H_2 < z < \sigma H_1$, in which ρ_0 is the characteristic density.

Solving (16) in each layer and ensuring $w = 0$ (hence $\psi = 0$) at the upper and lower boundaries, we find

$$\hat{\psi}(z) = \begin{cases} A_1 \sinh[k(H_1 - z)] & \sigma H_1 < z \le H_1 \\ B_1 \sin(mz) + B_2 \cos(mz) & -\sigma H_2 \le z \le \sigma H_1 \\ C_1 \sinh[k(z + H_2)] & -H_2 \le z < -\sigma H_2, \end{cases} \qquad (22)$$

in which m is given by (17). The constants A_1, B_1, B_1 and C_1 are interrelated through conditions at $z = \sigma H_1$ and $z = -\sigma H_2$ that require continuity of pressure and vertical velocity. In the absence of background shear, this amounts to continuity of $\hat{\psi}(z)$ and its derivative. Thus we have an eigenvalue problem formed from the four equations in the four unknown constants.

After some algebra, we derive the following implicit formula for m:

$$\tan(mH\sigma) = -\frac{m}{k} \left(\tanh[kH_1(1 - \sigma)] + \tanh[kH_2(1 - \sigma)] \right) \times$$
$$\left(1 - \frac{m^2}{k^2} \tanh[kH_1(1 - \sigma)] \tanh[kH_2(1 - \sigma)] \right)^{-1}.$$
$$\simeq -mH(1 - \sigma) \left(1 - m^2 H_1 H_2 (1 - \sigma)^2 \right)^{-1}, \qquad (23)$$

where in the second expression we have made the long wave approximation $(kH \ll 1)$. As $\sigma \to 1$, corresponding to the limit of uniform stratification, we have $\tan mH \simeq 0$. Therefore
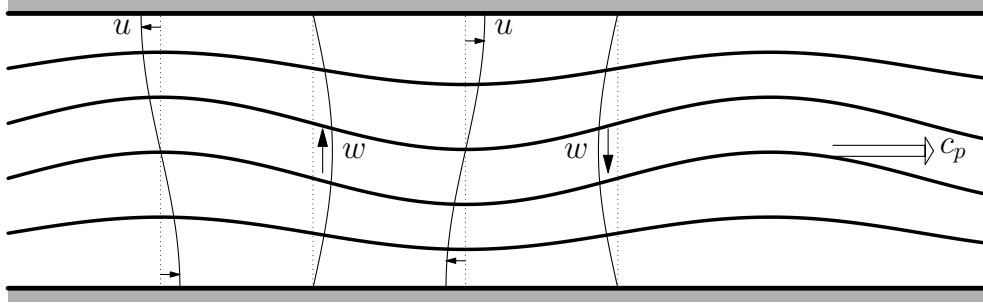
Figure 6: Schematic showing the velocity fields associated with a rightward-propagating mode-1 internal wave in a uniformly stratified fluid of finite depth.

m holds the values $m_i \equiv i\pi/H$, for integers i, as we found above. The corresponding dispersion relation is given by (19). As $\sigma \to 0$, corresponding to the limit of a two-layer fluid, we have $mH\sigma \simeq -mH/(1 - m^2 H_1 H_2) \simeq H/(mH_1H_2)$. That is, $m^2 H\sigma = 1/\bar{H}$, in which $\bar{H} = H_1 H_2/(H_1 + H_2)$ is the harmonic mean of the upper and lower-layer depths. Using this result in (19) with N_0 given by (21) and assuming $k \ll m$, we find $\omega^2 = g'\bar{H}k^2$, which is the dispersion relation for long waves given by (10).

In general, having found m through the empirical solution of (23) we can go on to find the interrelationship between the coefficients A_1, B_1, B_2 and C_1. Thus to within an arbitrary, though necessarily small, amplitude we have found the corresponding eigenfunction $\hat{\psi}(z)$. The polarization relations are then used to find the other fields of interest. In particular, from $w = \partial\psi/\partial x$ and the fact that the vertical displacement field ξ satisfies $w = \partial\xi/\partial t$, we have

$$\xi(x, z, t) = \hat{\xi}A\cos(kx - \omega t) \quad \text{with} \quad \hat{\xi}(z) = -\frac{k}{\omega}\hat{\psi}(z), \tag{24}$$

in which $\hat{\psi}$ is given by (22). Here we have defined A to be the maximum vertical displacement and it is implicitly assumed that the constants in $\hat{\psi}$ have been normalized so that $\hat{\xi}$ has a maximum value of unity.

Figure 7 shows the dispersion relation and vertical velocity amplitudes of the lowest vertical-mode internal waves for ambient profiles given by (20) with four different values of the interface thickness σH. So we see that in all three cases the vertical velocity is greatest in the interior of the domain with its value peaking closer to the mid-point of the interface at $z = 0$ as the interface becomes thinner ($\sigma \to 0$).

4 DISPERSION OF SMALL-AMPLITUDE WAVES

So far we have focused upon the structure and evolution of plane waves, with a single wavenumber and corresponding frequency. These are sometimes referred to as "monochromatic" waves. In reality, waves cannot be periodic out to infinity but have finite spatial extent. In many circumstances, however, the waves in a wavepacket have an approximately constant wavelength which is much smaller than the size of the wavepacket itself. This is

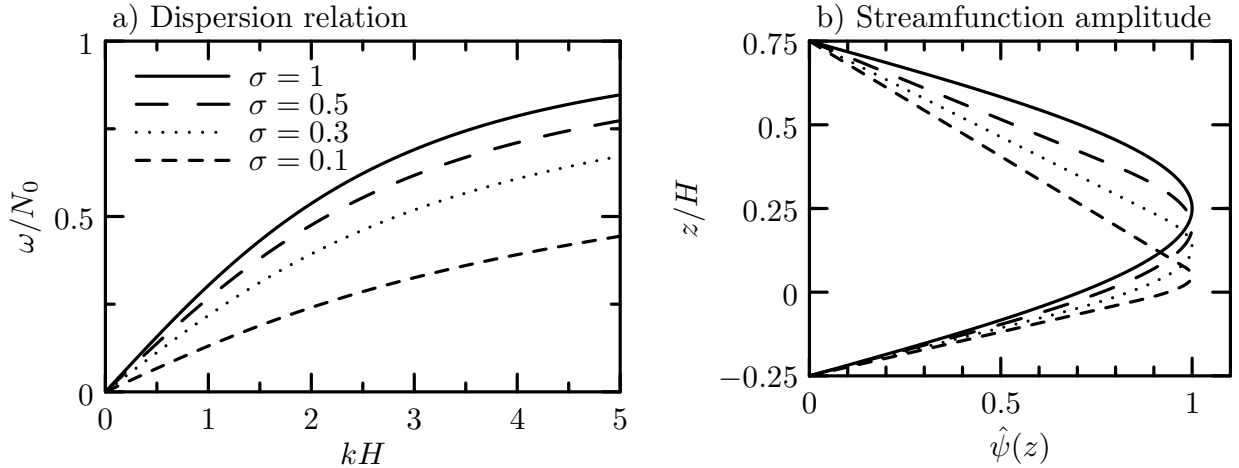a) Dispersion relation   b) Streamfunction amplitude

Figure 7: a) Dispersion relation of the lowest mode vertically-bounded internal waves in an ambient with density profile given by (20). The plots correspond to different interface thicknesses, σH with $H = H_1 + H_2$, as indicated. The upper and lower layers have relative depth $H_1/H = 0.75$ and $H_2/H = 0.25$, respectively. Frequency is normalized by the buoyancy frequency of the interface N_0 given by (21). b) Streamfunction amplitudes for the lowest mode with $kH = 0.1$ normalized so that its maximum value is unity. Each plot corresponds to different values of σ as indicated in a).

called a "quasi-monochromatic" wavepacket because it behaves similarly to monochromatic waves.

For simplicity, we will consider the evolution of a horizontally propagating packet of interfacial waves, though we will see in Section 6 how these ideas extend to describe vertically propagating internal wavepackets. The initial interface displacement field of a quasi-monochromatic wavepacket is represented by

$$\eta(x,0) = A(x,0)\cos(k_0 x),$$

in which the amplitude is not constant but varies in the horizontal as $A(x, t = 0)$. This describes the initial amplitude envelope of the wavepacket. For example, a Gaussian wavepacket centred at the origin has $A(x,0) = A_0 \exp(-x^2/2L^2)$ in which L is the width of the wavepacket. In the limit of infinitely large L, $A(x,0) \to A_0$ and we recover the representation of plane waves having wavenumber k_0.

In what follows, it is more convenient to write η in terms of complex exponentials through

$$\eta(x,z,0) = \frac{1}{2}A(x,0)e^{\imath k_0 x} + c.c. = \Re\{Ae^{\imath k_0 x}\}, \tag{25}$$

in which $c.c.$ denotes the complex conjugate of the first expression on the right-hand side of (25) and the symbol $\Re$ denotes the real-part of the expression it contains. Adding the complex conjugate has the effect of eliminating the imaginary part and doubling the real part. Because $e^{\imath\theta} = \cos\theta + \imath\sin\theta$ we recover $\eta = A\cos(k_0 x)$ if A is real-valued. If $A = A_r + \imath A_i$ is complex-valued, then its argument $\phi(x) = \tan^{-1}(A_i/A_r)$ describes the variation in space of the phase of the waves.

The horizontal structure of the wavepacket can be seen as the superposition of plane waves through the Fourier transform

$$\eta(x,0) = A(x,0)e^{\imath k_0 x} = \int_{-\infty}^{\infty} \hat{\eta}(k)e^{\imath k x}\, dk, \tag{26}$$

in which the amplitude of the plane wave with wavenumber k is

$$\hat{\eta}(k) = \frac{1}{2\pi}\int_{-\infty}^{\infty}\left(A(x,0)e^{\imath k_0 x}\right)e^{-\imath k x}\, dx. \tag{27}$$

In (26) we have adopted the convention that η is the real part of the expression on the left-hand side without explicitly writing the symbol $\Re$.

For example, in the case of the Gaussian wavepacket we have

$$\hat{\eta}(k) = (\sqrt{2\pi}\, L)A_0 \exp\left[-L^2\frac{(k_0-k)^2}{2}\right].$$

The amplitude is largest if $k = k_0$, the wavenumber of waves contained within the amplitude envelope. If $|k_0 - k| \gg 1/L$ the waves have negligible amplitude. So, although the wavepacket is a superposition of the whole spectrum of waves, only those with wavenumber near k_0 have any significant contribution to the structure of the waves.

For small-amplitude waves, each plane wave component of the wavepacket evolves in time through the change in the phase $-\omega t$. That is

$$\eta(x,t) = \int_{-\infty}^{\infty}\hat{\eta}(k)e^{\imath(kx-\omega t)}\, dk, \tag{28}$$

in which $\hat{\eta}$ is given by the initial condition (27) and $\omega = \omega(k)$ is itself a function of k through the dispersion relation.

For non-dispersive waves the dispersion relation is $\omega = ck$ with c constant. Substituting this into (28) and using (26), we immediately find $\eta(x,t) = \eta(x-ct,0)$; the waves translate at speed c without change in structure of the initial wavepacket.

For dispersive waves the phase speed ω/k is not independent of k. So different wavelengths propagate at different speeds and this results in a change of the shape of the wavepacket through a process referred to as "dispersion".

The effect of dispersion is described by the evolution of the amplitude envelope in time. We implicitly define the amplitude envelope, $A(x,t)$, of the evolving wavepacket by

$$\eta(x,t) = A(x,t)e^{\imath(k_0 x - \omega_0 t)}, \tag{29}$$

in which $\omega_0 = \omega(k_0)$ is the frequency of plane waves contained within the wavepacket and it is understood η is the real part of the right-hand side of (29). Substituting this into (28) and isolating A gives an integral expression for the amplitude envelope:

$$A(x,t) = \int_{-\infty}^{\infty}\hat{\eta}(k)e^{\imath[(k-k_0)x-(\omega(k)-\omega_0)t]}\, dk, \tag{30}$$

Given $\hat{\eta}(k)$ and the dispersion relation $\omega(k)$, the integral can be evaluated numerically and the interface displacement at any time is then given by $\Re\{A(x,t)\exp[\imath(k_0 x - \omega_0 t)]\}$.

Insight into the evolution of A is found by noting that for a quasi-monochromatic wavepacket $\hat{\eta}$ is negligibly small except where $k \simeq k_0$. This inspires us to perform a Taylor series expansion of ω about $k = k_0$. Truncating at third-order in $k - k_0$ gives

$$\omega(k) \simeq \omega_0 + \omega'(k_0)(k - k_0) + \frac{1}{2}\omega''(k_0)(k - k_0)^2 + \frac{1}{6}\omega'''(k_0)(k - k_0)^3$$

Substituting this into (30) gives a seemingly ugly expression. But nice things happen upon taking derivatives on both sides of the expression. Taking a time derivative brings a factor $-\imath\omega'(k - k_0) - \frac{\imath}{2}\omega''(k - k_0)^2 - \frac{\imath}{6}\omega''(k - k_0)^3$ into the integrand and taking successive x-derivatives brings factors $\imath(k - k_0)$, $-(k - k_0)^2$ and $-\imath(k - k_0)^3$ into the integrand. Thus we may combine these results to eliminate the integrals on the right-hand side leaving an equation that relates time and space derivatives:

$$\frac{\partial A}{\partial t} + \omega'(k_0)\frac{\partial A}{\partial x} - \frac{\imath}{2}\omega''(k_0)\frac{\partial^2 A}{\partial x^2} - \frac{1}{6}\omega'''(k_0)\frac{\partial^3 A}{\partial x^3} = 0. \tag{31}$$

The first two terms on the left-hand side describe the translation of the amplitude envelope at speed $\omega'(k_0)$. So we have shown that the wavepacket translates at the group speed $c_g = \omega'(k_0)$. The third term on the left-hand side of (31) shows that the amplitude-envelope changes in time where it has greater curvature. This describes the dispersion of the wavepacket. In some cases the coefficient $\omega''(k_0) \simeq 0$ in which case the fourth term on the left-hand side of (31) describes the dominant influence of dispersion.

Equation (31) is an extension of the well-known Schrödinger equation. The usual form of this equation neglects that last term on the left-hand side and is written in a frame of reference $X = x - c_g t$ moving at the group velocity. Hence

$$\frac{\partial A}{\partial t} = \frac{\imath}{2}\omega''(k_0)\frac{\partial^2 A}{\partial X^2}. \tag{32}$$

For a non-dispersive wave with $\omega = ck$, $c_g = c$ and $\omega''(k) = 0$. So a wavepacket translates at the same speed as the phase speed and does not disperse. For interfacial waves that are long, but not too long, the dispersion relation (9) for rightward-propagating waves is given approximately for small k by

$$\omega \simeq ck - \frac{1}{6}cH_1 H_2 k^3, \tag{33}$$

in which c is the long wave speed, as given below (10). Substituting this into (31), thereby gives an equation describing the evolution of the amplitude envelope of moderately long interfacial waves:

$$\frac{\partial A}{\partial t} + c\frac{\partial A}{\partial x} + \frac{1}{6}cH_1 H_2\frac{\partial^3 A}{\partial x^3} = 0. \tag{34}$$

In this case the dispersion is given by third-order spatial derivatives of A. For shorter waves, $\omega''(k_0)$ is non-zero so the second-order spatial derivatives in (31) dominate dispersion.

Likewise, for vertically propagating internal waves in uniformly stratified fluid, the dispersion in z of a horizontally periodic, vertically localized wavepacket with peak vertical wavenumber m_0 is given by the equation for the amplitude envelope $A(z, t)$:

$$\frac{\partial A}{\partial t} + \omega_m(m_0)\frac{\partial A}{\partial z} - \frac{\imath}{2}\omega_{mm}(m_0)\frac{\partial^2 A}{\partial z^2} = 0. \tag{35}$$

Here the m subscripts denote derivatives of ω with respect to the vertical wavenumber in which ω given by the dispersion relation (19). The second term in (35) describes the vertical translation of the wavepacket at the group velocity $c_g = \partial\omega/\partial m$. Dispersion is given at leading order by the A_{zz} term which is valid provided $\omega_{mm} \neq 0$; the waves do not move near the fastest vertical group speed. Because the coefficient of the third term on the left-hand side of (35) is complex, we see that the curvature of the amplitude envelope first acts to change the relative phase of the waves and this then changes the magnitude of the amplitude.

5 INTERNAL SOLITARY WAVES

5.1 Solitary Waves in a two-layer fluid

The term solitary wave originally referred to a single hump-shaped, moderately large amplitude wave that travels faster than the long wave speed and maintains its shape due to a balance between linear dispersion, which tends to spread out the wave, and nonlinear steeping, which tends to sharpen the wave crests. Its evolution in terms of the surface displacement, η, was originally formulated for surface waves through the Korteweg-de Vries (KdV) equation

$$\eta_t + c_0\eta_x + \frac{3c_0}{2H}\eta\,\eta_x + \frac{1}{6}c_0 H^2 \eta_{xxx} = 0, \tag{36}$$

in which $c_0 = \sqrt{gH}$ is the shallow water wave speed based upon gravity, g, and the water depth H. Consistent with (34), the second and fourth terms on the left-hand side of (36) describes the advection and linear dispersion of the wavepacket. The third (nonlinear) term of (36) describes the steepening of the wave, an effect that is larger for waves of larger amplitude.

The solution of (36) for waves that have no upstream or downstream disturbance is

$$\eta = A\,\mathrm{sech}^2\left(\frac{x - Ut}{\lambda}\right), \tag{37}$$

in which width of the solitary wave is

$$\lambda = \sqrt{\frac{4H^3}{3A}} \tag{38}$$

and its speed is

$$U = c_0\left(1 + \frac{1}{2}\frac{A}{H}\right). \tag{39}$$

This last formula confirms that solitary waves propagate faster than the fastest speed c_0 associated with long, small-amplitude waves.

In (37), A is the amplitude of the wave which measures the maximum deflection of the surface from its far-upstream depth. Unlike small-amplitude waves, the speed of a solitary wave increases as the amplitude increases. Also, the width of the wave changes as $H\sqrt{H/A}$; it has narrower extent as the amplitude increases relative to the fluid depth H.

The KdV equation has been adapted to describe internal solitary waves in stratified fluid(Benney 1966; Grimshaw, Pelinovsky and Poloukhina 2002). In this case the vertical
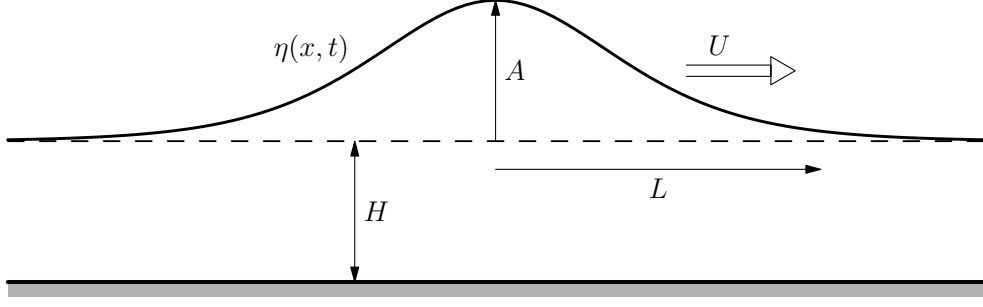
Figure 8: Schematic showing the structure of a solitary wave in a one-layer fluid of upstream-depth H. The surface displacement is represented by η with the maximum surface displacement being A.

displacement field η, which describes the displacement of isopycnals, is a function of z as well as x and t. Seeking the description of waves that propagate at constant speed, we assume η is separable so that we can write

$$\xi(x, z, t) = \hat{\xi}(z)\eta(x, t). \tag{40}$$

For example, in the small-amplitude limit for mode-1 waves in uniformly stratified fluid, we would have $\hat{\xi}(z) = \sin(m_1 z)$ and $\eta(x, t) = A\cos(kx - \omega t)$ (see Table 2). So, just as η describes the displacement of the interface for waves in a two-layer fluid, here η describes the maximum isopycnal deflection over the vertical extent of the domain. For the case of small-amplitude internal waves at a thick interface given by (20), the vertical displacement field is given by (24). That is $\hat{\xi}(z) = -(k/\omega)\hat{\psi}$ with $\hat{\psi}$ given by (22), normalized so that $\max(\hat{\xi}) = 1$.

For moderately large amplitude waves, we assume the vertical mode structure is unchanged from the linear theory values and so derive a formula that describes modification in $\eta(x, t)$ from sinusoidal behaviour due to weakly nonlinear effects.

In general, the evolution equation

$$\eta_t + c_0\eta_x + \alpha\eta\ \eta_x + \beta\eta_{xxx} = 0, \tag{41}$$

in which c_0 is the long wave speed from linear theory and the constants α and β are given in terms of vertical integrals over the domain of $\hat{\xi}$:

$$\alpha = \frac{3}{2}c_0\frac{\int \bar{\rho}(\hat{\xi}')^3\, dz}{\int \bar{\rho}(\hat{\xi}')^2\, dz} \quad \text{and} \quad \beta = \frac{1}{2}c_0\frac{\int \bar{\rho}\hat{\xi}^2\, dz}{\int \bar{\rho}(\hat{\xi}')^2\, dz}, \tag{42}$$

in which the primes denote z-derivatives. A generalization of these coefficient formulae that include background vertical shear was first determined by (Benney 1966) and later extended by (Grimshaw, Pelinovsky and Poloukhina 2002) to include higher-order nonlinear forcing terms and allowing for a free surface. In the Boussinesq approximation, the ambient density profile, $\bar{\rho}(z)$, can be taken as constant so eliminating the density from the integrals altogether.
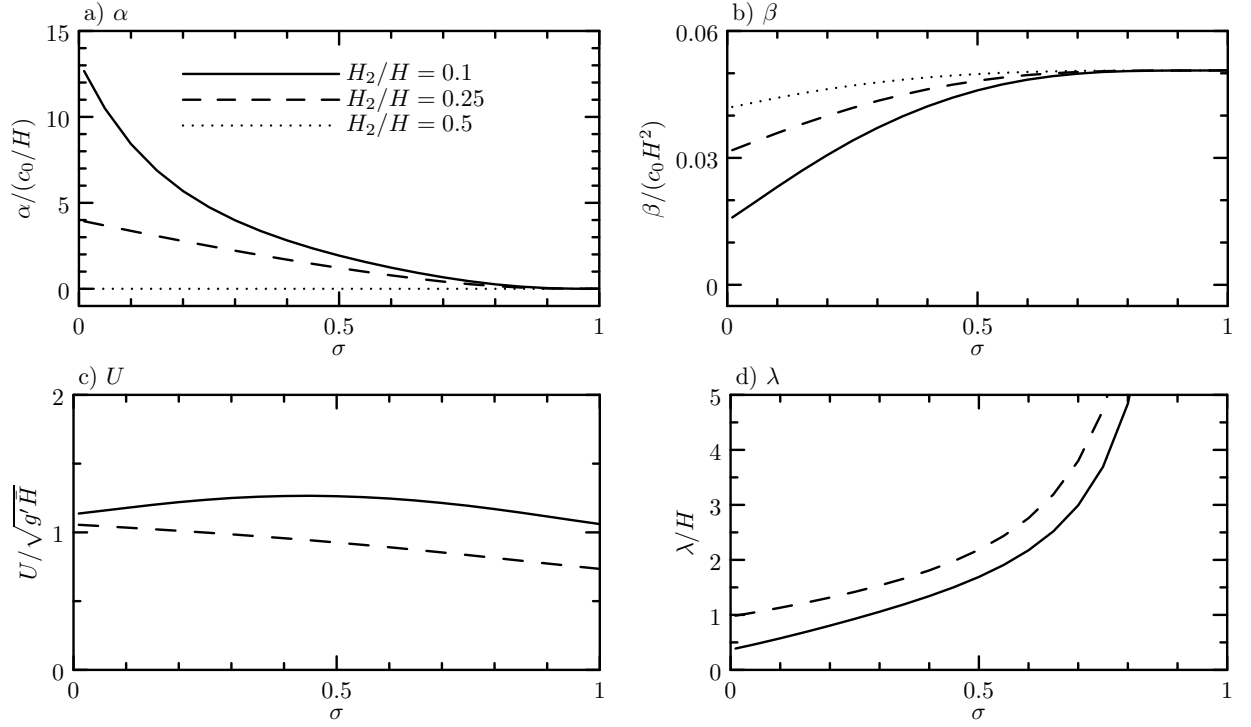
15

Figure 9: Numerically calculated coefficients of a) α and b) β in the KdV equation computed for the lowest mode of a shallow wave with $kH = 0.1$ in a fluid with ambient stratification given by (20). The corresponding c) speed U computed for $A = 0.1H$ and d) width λ of the wave. Values are given as a function of the relative thickness of the interface, σ, for different relative lower layer thicknesses H_2/H as indicted in a). Note, the speed and width of the wave are shown only for $H_2/H = 0.1$ and 0.25, for which solitary wave solutions exist.

As for a one-layer fluid, the solution of (41) having no upstream or downstream displacement is given by (37) except now the width and speed of the solitary wave is given by

$$\lambda = \sqrt{\frac{12\beta}{A\alpha}} \tag{43}$$

and

$$U = c_0 \left(1 + \frac{1}{3}A\alpha \right), \tag{44}$$

respectively. This can be confirmed through substitution of (37) into (41).

In particular, for a two-layer fluid, Table 1 gives $\hat{\xi} = 1 - z/H_1$, for $0 < z \le H_1$, and $\hat{\xi} = 1 + z/H_2$, for $-H_2 \le z \le 0$. So (42) gives

$$\alpha = \frac{3}{2}c_0 \frac{-\frac{\rho_1}{H_1{}^2} + \frac{\rho_2}{H_2{}^2}}{\frac{\rho_1}{H_1} + \frac{\rho_2}{H_2}} \quad \text{and} \quad \beta = \frac{1}{6}c_0 \frac{\rho_1 H_1 + \rho_2 H_2}{\frac{\rho_1}{H_1} + \frac{\rho_2}{H_2}} \tag{45}$$

For a one-layer fluid ($\rho_1 \to 0$), these reduce to $\alpha = 3c_0/2H_2$ and $\beta = c_0 H_2{}^2/6$, consistent

with the coefficients in (36). Substituting these into (43) and (44) gives the width and speed and the solitary wave consistent with (38) and (39).

In the Boussinesq approximation, where the density difference between the upper and lower layers is small (45) simplifies to

$$\alpha = \frac{3}{2} c_0 \frac{H_1 - H_2}{H_1 H_2} \quad \text{and} \quad \beta = \frac{1}{3} c_0 H_1 H_2. \tag{46}$$

In particular, we see that $\alpha = 0$ if $H_1 = H_2$. That is, the effect of nonlinear steepening as it is captured by the KdV equation vanishes if the upper and lower layer depths are equal. This is true even if the interface between the two fluids has finite thickness, as shown in Figure 9.

Although the speed and spatial-scale of the wave changes with amplitude, the sech-squared shape does not. However, observations show that the crests of internal solitary waves tend to flatten as they grow to large amplitude. This effect has been captured in the so-called extended KdV equation, which includes higher order linear and nonlinear dispersion effects (Lee and Beardsley 1974; Lamb and Yan 1996; Grimshaw, Pelinovsky and Poloukhina 2002).

6   WEAKLY NONLINEAR INTERNAL WAVES

In an unbounded stratified fluid internal waves can propagate vertically as well as horizontally, as discussed for small-amplitude waves in section 3. Here we will examine how the evolution of the waves changes when they have moderately large amplitude. We will focus upon two-dimensional horizontally periodic internal waves in a uniformly stratified Boussinesq fluid that have limited vertical extent. Unlike horizontally propagating solitary waves which exist in steady state through a balance between nonlinear steepening and linear dispersion, we will show that weakly nonlinear effects cause the shape of the amplitude envelope of internal waves to change, either spreading out faster than linear dispersion predicts or narrowing and growing in amplitude.

As discussed in Section 4, the evolution of a horizontally periodic, vertically localized wavepacket can be described in terms of the change in the amplitude envelope $A(z,t)$ through (48). For a wavepacket with central wavenumber $\vec{k}_0 = (k_0, m_0)$ and initial vertical displacement field $\Re\{A(z,0)\exp[\imath(k_0 x + m_0 z)]\}$, the displacement at a later time is

$$\xi(x,z,t) = \Re\left\{A(z,t)e^{\imath(k_0 x + m_0 z - \omega_0 t)}\right\} \tag{47}$$

in which $\omega_0 = \omega(k_0, m_0)$ is the dispersion relation given by (19) and the amplitude envelope changes in time according to (35). In a frame of reference moving at the vertical group speed this equation is

$$\frac{\partial A}{\partial t} = \frac{\imath}{2} \gamma \frac{\partial^2 A}{\partial Z^2}, \tag{48}$$

in which $Z = z - c_g t$, $c_g \equiv \omega_m(m_0) = -N_0 m_0 k_0 / |\vec{k}_0|^{3/2}$, and $\gamma \equiv \omega_{mm}(m_0) = N_0 k_0 (2m_0^2 - k_0^2) / |\vec{k}_0|^{5/2}$.

Horizontally periodic internal waves induce a mean flow, akin to the Stokes drift of surface waves. It turns out that the weakly nonlinear evolution of vertically propagating
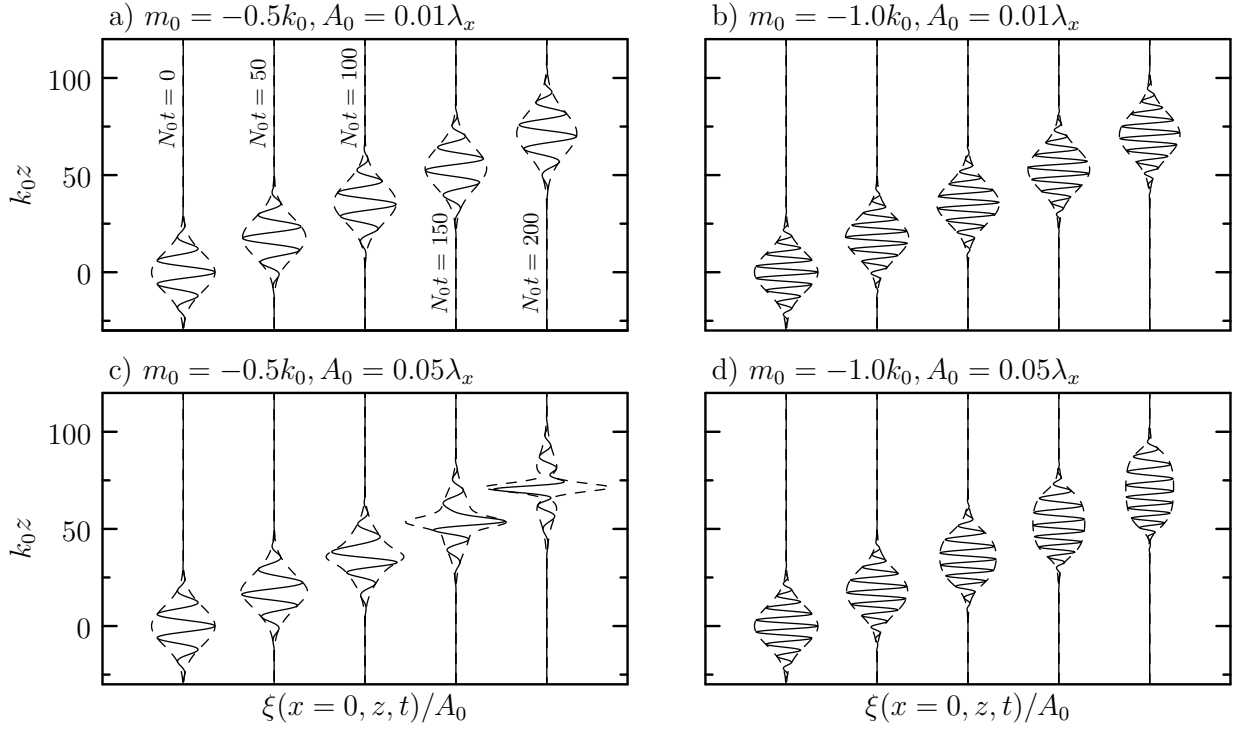
Figure 10: Numerically computed solution of (51) giving the evolution of a vertically propagating internal wavepacket with relatively small initial vertical displacement amplitude, A_0, and central vertical wavenumber a) $m_0 = -0.5k_0$ and b) $m_0 = -k_0$, and with moderately large initial amplitude and wavenumbers c) $m_0 = -0.5k_0$ and d) $m_0 = -k_0$. The initial amplitude envelope is a Gaussian centred at the origin with width $L = 10k_0^{-1}$. The waves propagate upward in uniformly stratified fluid with buoyancy frequency N_0. In each plot, horizontally offset profiles of the normalized vertical displacement are shown at the five times indicated in a).

internal waves is determined primarily through interactions between the waves and this mean flow, which we will denote by $\langle u \rangle_L$. The mean flow acts to advect the waves horizontally just as a background ambient flow would. Including the effects of this advection is done simply by replacing x in (47) with $x + \langle u \rangle_L t$. And so at leading-order, the time-derivative of ξ introduces a new term $\imath k_0 \langle u \rangle_L \xi$. This adjusts the evolution equation (48) for the amplitude envelope so that

$$\frac{\partial A}{\partial t} = \frac{\imath}{2}\gamma\frac{\partial^2 A}{\partial Z^2} - \imath k_0 \langle u \rangle_L A. \tag{49}$$

It remains to find an explicit expression for $\langle u \rangle_L$ in terms of the amplitude A. From the horizontal momentum equation (11), if we expand out the material derivative and average horizontally over one wavelength we get $\partial_t \langle u \rangle_L = -\partial_z \langle uw \rangle$; the flow accelerates due to the divergence in the vertical flux of horizontal momentum per unit mass. In this case the flux changes with height because the amplitude envelope changes in the vertical. Far above and below the wavepacket there is no flux because there are no waves whereas the flux is large

at the centre of the wavepacket. Knowing that the wavepacket moves upwards at the group speed c_g, we can write $\partial_t \langle u \rangle_L + c_g \partial_z \langle u \rangle_L \simeq 0$. Thus we have $\langle u \rangle_L = \langle uw \rangle / c_g$. Finally, if we use the polarization relations in Table 2 that relate the horizontal and vertical velocity amplitudes for vertically propagating waves to the vertical displacement, we have

$$\langle u \rangle_L = -\frac{1}{2c_g} |A|^2 {\omega_0}^2 \frac{m_0}{k_0} . = \frac{1}{2} N_0 |\vec{k}_0| |A|^2 . \tag{50}$$

Putting this result into (49), we have the weakly nonlinear evolution equation for vertically propagating internal wavepackets

$$\frac{\partial A}{\partial t} = \frac{1}{2} \imath \gamma \frac{\partial^2 A}{\partial Z^2} - \imath \omega_2 |A|^2 A, \tag{51}$$

in which $\omega_2 = N_0 |\vec{k}_0| k_0 / 2$ is the finite-amplitude correction to the dispersion relation: $\omega = \omega_0 + \omega_2 |A|^2$. Equation (51), generally known as a "nonlinear Schrödinger equation", describes the evolution of finite-amplitude dispersive wavepackets.

Given an initial amplitude envelope $A(z,0)$, (51) describes how the amplitude and phase of the wavepacket changes in time through changes to the real and imaginary part of $A(z,t)$. Extracting the real part of $A(z,t) \exp[\imath(k_0 x + m_0 z - \omega t)]$ gives the vertical displacement field ξ. This is shown in Figure 10 for small and large amplitude wavepackets having relative vertical wavenumbers of $m_0 = -0.5k_0$ and $m_0 = -k_0$. With $k_0 > 0$, the negative sign assures that the wavepacket propagates upward.

The figure shows that wavepackets having initial maximum amplitude as small as one-percent of the horizontal wavelength ($A_0 = 0.01\lambda_x$) undergo linear dispersion as would be predicted by (35). The influence of the nonlinear term in (51) is evident for waves having amplitude $A_0 = 0.05\lambda_x$. Depending upon the vertical wavenumber, the wavepacket either narrows and grows in amplitude ($m_0 = -0.5k_0$) or it broadens more quickly than linear theory predicts ($m_0 = -k_0$). In the former case the waves are said to be "modulationally unstable" and in the latter case the waves are "modulationally stable".

The transition from instability to stability occurs for wavepackets with m_0 satisfying $\omega_{mm}(m_0) = 0$. Explicitly, this occurs when $|m_0| = |k_0|/\sqrt{2}$, corresponding to waves of fixed k_0 moving at the fastest vertical group velocity (Sutherland 2006b).

The consequent dynamics of large amplitude internal waves is not as well captured by (51). The growth in amplitude of modulationally unstable wavepackets means that higher-order terms in the nonlinear Schrödinger equation, which we have neglected, have a non-negligible contribution to the wavepacket evolution. At later times still, wave-wave interaction give rise to superharmonic waves through what is known as parametric subharmonic instability (Sutherland 2006a). A detailed investigation of these weakly and fully nonlinear dynamics upon the evolution of large-amplitude internal wavepackets remains under investigation.

7   CONCLUSIONS

In this chapter we have attempted to draw the connection and distinctions between finite-amplitude interfacial waves that propagate horizontally in a vertically confined domain

and internal waves that propagate vertically in unbounded uniformly stratified fluid. The evolution of the former is given by the KdV equation (41) whereas that of the latter is prescribed by the nonlinear Schrödinger equation (51).

Generally, the KdV equation describes moderately long amplitude waves that have permanent form while translating at a speed moderately larger than the speed of long interfacial waves. Examination of this equation provides a useful starting point in understanding the dynamics of internal solitary waves such as those generated by tidal flows over sills and the continental shelf. However, the equation makes approximations that assume the amplitude is not too large. To describe internal solitary waves of large amplitude, higher order terms can be included as in the Extended KdV equation, which predicts the wave crests flatten (Helfrich and Melville 2006). At larger amplitude still, the solitary waves can develop closed cores in which fluid is transported along with the wave. Such dynamics have been described by a different approach through the solution of the Dubreil-Jacotin-Long equation (Long 1953; Dubreil-Jacotin 1937; Brown and Christie 1998). These considerations lie beyond the scope of the material presented here.

Generally, the nonlinear Schrödinger equation describes the influence of large-amplitude effects upon dispersive waves. Rather than providing steady state solutions for wavepackets, the equations predict that the amplitude envelope of the waves spread or narrow from their initial state. Spreading, modulationally stable, waves occur if $\omega_2 \omega'' > 0$, in which ω_2 is the order amplitude-squared correction to the frequency ω predicted for small-amplitude waves. For internal waves, this occurs if the magnitude of the vertical wavenumber $|m_0|$ exceeds $|k_0|/\sqrt{2}$ in which $|k_0|$ is the magnitude of the horizontal wavenumber. The implications of this result remain to be explored. At first glance it would seem that large-amplitude internal waves should break at higher levels because the amplitude decreases as the wavepacket spreads nonlinearly. However, nonlinear effects neglected by the nonlinear Schrödinger equation may introduce other modes of instability that could cause breaking at lower levels. Whatever the case these results show that wave breaking in the atmosphere assessed by extrapolation of linear theory, likely incorrectly predicts where momentum is actually deposited by the waves.

References

Benney, D. J. 1966. Long nonlinear waves in fluid flows. *J. Math. and Phys.*, 45:52–63.

Brown, D. J. and Christie, D. R. 1998. Fully nonlinear solitary waves in continuously stratified incompressible boussinesq fluids. *Phys. Fluids*, 10:2569–2586.

Dubreil-Jacotin, M. L. 1937. Sur les théoremes d'existence relatifs aux ondes permanentes pérodiques à deux dimensions dans les liquides hétérogènes. *J. Math. Pures Appl.*, 16:43–67.

Grimshaw, R. H. J., Pelinovsky, E., and Poloukhina, O. 2002. Higher-order Korteweg-de Vries models for internal solitary waves in a stratified shear flow with a free surface. *Nonlin. Proc. Geophys.*, 9:221–235.

Helfrich, K. R. and Melville, W. K. 2006. Long nonlinear internal waves. *Annu. Rev. Fluid Mech.*, 38:395–425.

Lamb, K. G. and Yan, L. 1996. The evolution of interanl wave undular bores: Comparison of a fully-nonlinear numerical model with weakly nonlinear theories. *J. Phys. Oceanogr.*, 26:2712–2734.

Lee, C.-Y. and Beardsley, R. 1974. The generation of long nonlinear internal waves in a weakly stratified shear flow. *J. Geophys. Res.*, 79:453–462.

Long, R. R. 1953. Some aspects of the flow of stratified fluids. a theoretical investigation. *Tellus*, 5:42–58.

Sutherland, B. R. 2006a. Internal wave instability: Wave-wave vs wave-induced mean flow interactions. *Phys. Fluids.*, 18:Art. No. 074107. doi:10.1063/1.2219102.

Sutherland, B. R. 2006b. Weakly nonlinear internal wavepackets. *J. Fluid Mech.*, 569:249–258.

Sutherland, B. R. 2010. *Internal Gravity Waves*. Cambridge University Press, Cambridge, UK.

Troy, C. D. and Koseff, J. R. 2005. The instability and breaking of long internal waves. *J. Fluid Mech.*, 543:107–136.